Polymer Bulletin
https://doi.org/10.1007/s00289-025-05993-z

ORIGINAL PAPER

Fracture mechanics of thermoplastic elastomers: applicability of the load separation criterion

Stefano Gozzini[1] · Jacopo Agnelli[1] · Silvia Agnelli[1] · Fabio Bignotti[1] · Alessandro Rasetta[2] · Francesco Baldi[1]

Received: 13 June 2025 / Revised: 30 July 2025 / Accepted: 19 August 2025
© The Author(s) 2025

Abstract

Initially proposed for metals and then extended to polymeric materials, the Load Separation Criterion, LSC, is the theoretical basis of several laboratory test methods for the fracture characterisation of materials exhibiting plasticity. In this work, the applicability of the LSC to the fracture characterisation of thermoplastic elastomers, TPEs, was analysed and discussed for the first time. Due to their peculiar nature, TPEs combine melt state processability with a high compliance and elasticity typical of rubbers. At a macroscopic scale, their mechanical response appears generally complex, with an evident viscoelastic character coupled with clear signs of plasticity (behaviour often referred to as of the elastoviscoplastic type). Three industrially relevant TPEs, differing for the chemical nature, were examined. First, their stress-strain behaviour was studied by uniaxial tensile tests, carried out on dumbbell specimens. Then, to verify the load separability, single-edge notched in tension, SENT, tests were carried out on blunt-notched specimens (stationary crack tests under plane stress conditions). Specimens with different crack-length/width ratios were tested at room temperature and with a fixed crosshead speed (low rate). The LSC proved to be valid for all three TPEs studied.

Keywords Fracture mechanics · Load separation criterion · Single-edge notched in tension specimens (SENT) · Stress-strain behaviour · Thermoplastic elastomers (TPEs)

✉ Francesco Baldi
francesco.baldi@unibs.it

[1] Dipartimento di Ingegneria Meccanica e Industriale, Università degli Studi di Brescia, Via Branze 38, 25123 Brescia, Italy

[2] Univet S.r.l., Via G. Prati 87, 25086 Rezzato, Italy

Published online: 03 September 2025

Introduction

The quantification of materials' fracture toughness is a key step to ensure structural integrity of components. The application of fracture mechanics enables the structural analysis of imperfect bodies with well-known flaws and provides fracture criteria that take into account the stress intensification that a crack raises. Real parts have cracks because of things like mistakes in the production process or damage that happens during use (like scratches). Cracks make the stress level in the material worse because they cause both stress intensification and stress triaxiality. Failure criteria therefore rely on fracture mechanics parameters to quantify materials' resistance to fracture (fracture toughness).

In the late 1960s, Cherepanov [1] and Rice [2] proposed the J-integral for both linear and nonlinear elastic materials, which is one of the many fracture mechanics parameters. It was derived by extending the energy release rate concept of Linear Elastic Fracture Mechanics, LEFM, to a nonlinear elastic material behaviour, and it is used also for ductile materials with an elastic–plastic response (within the frame of Elastic–Plastic Fracture Mechanics, EPFM) [3].

The original method for the experimental evaluation of the J-integral values was proposed by Begley and Landes [4, 5]. It was a very accurate method, but, being a multi-specimen approach, it had the disadvantage of requiring many specimens to be tested; furthermore, it did not propose a general expression for J-calculation (the measured J-values were valid only for the specific material, specimen size and geometry used to obtain them). In an effort to identify alternative techniques to simplify J-calculation, the attention was focused on single-specimen approaches founded on the load separability concept proposed by Ernst et al. [6] in 1981 and further developed by Sharobeam and Landes in the early nineties [7, 8]. According to this concept (known as Load Separation Criterion, LSC), in a fracture test, for a defined specimen geometry, material, and constraint, in the plastic region, the load, P, can be mathematically represented in a separable form as the multiplication of two independent functions, a geometry function, G, and a material deformation function, H, as in the following expression:

$$P = G\left(\frac{b}{W}\right) \cdot H\left(\frac{u_{\mathrm{pl}}}{W}\right) \tag{1}$$

where b is the uncracked ligament length, W the specimen width, and u_{pl} the plastic displacement. The plastic displacement is the plastic component of the total displacement, u, and is given by:

$$u_{\mathrm{pl}} = u - P \cdot C\left(\frac{b}{W}\right) \tag{2}$$

where $C(b/W)$ is the elastic compliance of the tested specimen. G is a function depending only on specimen geometry, whereas H is a function only of material and constraint.

Proposed for metals (and verified for several testing configurations, including single-edge notched in bending, SENB, and single-edge notched in tension, SENT), the

applicability of the LSC was subsequently demonstrated also for polymeric materials, in SENB tests, both during the blunting and the crack propagation phases (see [9–15]). For the fracture characterisation of polymeric materials exhibiting a ductile behaviour, several experimental methodologies theoretically based on the LSC have been used, such as the normalisation (see [9, 11–13, 16–18]) and the S_{pb} (see [14, 19]) methods. More recently, an LSC-based method aimed at measuring the initiation fracture toughness was developed by ESIS TC4 [20, 21], which is the Technical Committee 4, "Polymers, Polymer Composites and Adhesives", of the "European Structural Integrity Society" (ESIS) [22]. This method is at present under consideration as an ISO standard (with the title "Determination of fracture toughness (J_{Ic}) of ductile polymers: The load separation criterion-based method"), within Working Group 7 "Fracture and fatigue behaviour" of Sub-Committee 2 "Mechanical behaviour" of Technical Committee 61 "Plastics" [23].

So far, to the authors' knowledge, the LSC has never been applied to thermoplastic elastomers, TPEs. TPEs are an important class of polymeric materials, used in many applications spanning from medical to automotive, from electronics to construction fields. Shoe soles, mobile phone covers, diving masks, suspension bushings, and catheters are just a few examples of applications [24].

TPEs combine the melt processability of thermoplastics with the high elasticity and compliance of rubbers. They are multiphase materials, consisting of hard domains acting as physical crosslinks for the molecules of the soft phase. The hard phase is characterised by low extensibility and high glass transition temperature and/or crystalline melting point, whereas the soft phase is characterised by high extensibility and low glass transition temperature [25]. The intrinsic recycling potential stemming from their thermo-reversible network makes them an attractive alternative to thermosetting elastomers when looking for increasing circularity and sustainability. Depending on the macromolecular structure, TPEs can be classified into two main classes: segmented block copolymers (as, for example, the thermoplastic copolyester, TPC, and the styrenic block copolymers, TPS) and polymer blends (as, for example, the dynamically vulcanised blends, TPV).

The mechanical behaviour of TPEs depends on the molecular structure and shows: nonlinear elasticity with highly recoverable deformations, typical of a hyperelastic behaviour; time and temperature dependence, typical of viscoelastic materials; irreversible deformations, typical of elastoplastic materials; and energy dissipation upon unloading, as with filled rubbers [26, 27]. Moreover, the morphology of many TPEs may change during deformation and consequently also their mechanical properties [28]. The few works in the literature reporting fracture characterisations of TPEs adopt energy-based approaches to measure fracture toughness: the J-integral or the tearing energy to measure the energy release rate [29–31], or the essential work of fracture [29, 32]. In particular, the energy release rate is widely adopted to characterise fracture toughness of rubber since it allows circumventing the difficulty of finite strains and nonlinear elastic behaviour, and, as already mentioned, it may be applied both to nonlinear elastic and to elastic–plastic materials.

In this work, the applicability of the LSC to the fracture characterisation of TPEs was analysed. Three commercial grades of TPEs, differing in chemical nature, two of which are bio-based, were examined. The specimens for the

mechanical tests were obtained from ≈ 2 mm thick injection-moulded plates. First, their stress-strain behaviour was studied by performing uniaxial tensile tests on dumbbell specimens, both under monotonic and cyclic conditions. Then, to verify the load separability, stationary crack fracture tests were carried out on clamped SENT blunt-notched specimens (in plane stress conditions). For each TPE examined, the G and H functions, which are the basis of the LSC formulation, were constructed.

Theoretical background: applicability of the LSC

The validity of the LSC can be experimentally verified for a certain material, specimen geometry and constraint by testing at least two specimens with stationary cracks, i.e. not allowing for crack growth. This can be achieved, for example, by using blunt-notched specimens. The load separation parameter, S_{ij}, is defined as the ratio between the loads of two specimens with stationary crack lengths a_i and a_j at the same plastic displacement, u_{pl}:

$$S_{ij} = \left.\frac{P(a_i)}{P(a_j)}\right|_{u_{\mathrm{pl}}} \tag{3}$$

If the load can be represented in a separable form as in Eq. 1, taking into account that $b/W = (1 - a/W)$, then S_{ij} has a constant value independently of the level of plastic displacement examined, simply because:

$$S_{ij} = \left.\frac{P(a_i)}{P(a_j)}\right|_{u_{\mathrm{pl}}} = \left.\frac{G\left(1-\frac{a_i}{W}\right)\cdot H\left(\frac{u_{\mathrm{pl}}}{W}\right)}{G\left(1-\frac{a_j}{W}\right)\cdot H\left(\frac{u_{\mathrm{pl}}}{W}\right)}\right|_{u_{\mathrm{pl}}} = \left.\frac{G\left(1-\frac{a_i}{W}\right)}{G\left(1-\frac{a_j}{W}\right)}\right|_{u_{\mathrm{pl}}} \tag{4}$$

In other words, if S_{ij} is constant over the whole domain of u_{pl}, then the load can be represented by a separable form [7].

Moreover, for several test geometries, including the SENB and SENT [7], the geometry function can be represented by a power-law function:

$$G\left(\frac{b}{W}\right) = \left(\frac{b}{W}\right)^{\eta_{\mathrm{pl}}} \tag{5}$$

where η_{pl} is a geometry-dependent factor, which is used in the calculation of the J parameter with the following single-specimen form proposed by Sumpter and Turner [33]:

$$J = J_{\mathrm{el}} + J_{\mathrm{pl}} \tag{6}$$

where J_{el} equals the Griffith energy release rate [3], and J_{pl} can be evaluated by this expression:

$$J_{pl} = \eta_{pl} \frac{A_{pl}}{b} \tag{7}$$

where A_{pl} is the area under the load per unit thickness versus plastic displacement record. Paris et al. [34] found that this single-specimen J form and η_{pl} only exist if the load is separable. Therefore, another proof of the LSC validity is the fact that η_{pl}, calculated from the geometry function for a defined testing geometry, is not material dependent.

Experimental

The TPEs examined are presented in Table 1, which reports the brand name and producer of the materials, together with their TPE class, hardness (Shore A, according to ISO 868 [35]) and main transition temperatures (from Differential Scanning Calorimetry tests carried out with a TA Instruments Q100 calorimeter, using a scanning heating rate of 10 °C/min, under a nitrogen atmosphere). Materials B and C have a bio-based nature.

The materials, supplied in the form of pellets, were converted into plates (suitable for the obtainment of the specimens for the mechanical tests) by injection moulding, which is the processing technique they are intended for. A double-impression mould, with a $100 \times 60 \times 2$ mm^3 cavity fed through a film gate along the 60 mm edge, was used. For each TPE, the process parameters were chosen in such a way as to obtain regular quality parts, based on the indications provided by the material producer.

The specimens for the mechanical tests were taken directly from the plates in such a way as to ensure that the longitudinal axis of the specimen was parallel to the 100 mm edge of the plate. Up to three different specimens were taken from a single plate after having experimentally verified (results not shown here) that the specimen pickup point practically had no effect on the mechanical response of the material (within the standard deviation of the results). For the uniaxial tensile tests, dumbbell specimens according to ISO 37 "type-2" [36] (with a central narrow section with nominal width and length of 4 and 25 mm, respectively) were obtained by die-cutting. For the fracture mechanics tests, rectangular coupons with nominal width and

Table 1 Materials examined, their hardness and transition temperatures (from DSC tests, see text)

Material code	Brand name [producer]	TPE class	Hardness (Shore A, ISO 868)	Transition temperatures	
				Glass transition [°C]	Melting point [°C]
A	Santoprene™ [ExxonMobil]	TPV	80	-60	155
B	Arnitel™ [DSM]	TPC	92	-35	163
C	Chemiton™ [Franplast]	TPS compound	80	-60	124

length of 15 and 90 mm, respectively, were cut out by means of a well-sharpened laboratory cutter. The specimens had a thickness, B, of ≈ 2 mm.

The uniaxial tensile tests were performed by using the Instron test system 3366 equipped with a 500 N load cell at room temperature. The Instron video-extensometer AVE2 was used for the measurement of the nominal strain (engineering strain, indicated with elongation hereinafter, to better conform to the nomenclature proposed in ISO 37 [36]). Both monotonic (one-way) and cyclic (one single cycle) tests were carried out. In the monotonic tests the crosshead speed was set at 50 mm/min; in the cyclic tests it was set at 50 and 10 mm/min in the loading and unloading phase, respectively. From each test, the material nominal stress-elongation curve was obtained, with the nominal stress determined from the instantaneous values of the load normalised over the initial cross-section of the specimen in the narrow zone. For each specimen tested, the actual specimen thickness was measured by means of a 1 μm resolution micrometre. For each material, three specimens were analysed in the monotonic mode and one in the cyclic mode. In the cyclic tests, the "residual elongation" was taken as the value of the nominal strain corresponding to the first data point with a load below 0.1 N, measured during unloading. The "residual elongation at ∞ time" was measured after about ten weeks from the execution of the test.

For the fracture mechanics tests, SENT blunt-notched specimens were used. They were obtained by introducing at the middle of the 15×90 mm^2 coupons a key-hole type notch (see Fig. 1). A series of six different test pieces with notch length, a_0, to specimen width, W, ratios (a_0/W) between ≈ 0.2 and ≈ 0.8 were prepared for each TPE. The hole of the key-hole notch was obtained by die-cutting and had a nominal diameter of 2 mm. For each specimen, the actual thickness, B, was measured by means of a 1 μm resolution micrometre before notching; W and the uncracked ligament length, b_0, were measured on a photograph taken by a digital microscope, Leica DMS300, before the execution of the test.

The fracture tests were performed with the same machine used for the tensile tests, at room temperature and with a crosshead speed of 10 mm/min. A distance between the grips, h_0, of 40 mm was used. Although these tests were designed as stationary crack experiments, crack propagation was clearly noticed in most of the samples of materials A and B as the maximum load levels were approached, up to complete breakage. The tendency to show fracture propagation was much less marked for material C, for which all the tests were stopped before reaching the specimen breakage. In order to examine only portions of the loading curves where the test could be correctly considered as a stationary crack experiment, in the data processing, for a given material, the loading curves of all the specimens with the different a_0/W ratios were cut at a given displacement level.

Results and discussion

Both monotonic and cyclic uniaxial tensile tests were carried out to investigate the deformational behaviour of the materials. The stress-elongation curves from tensile tests, up to the specimen breakage, are shown in Fig. 2a. Table 2 shows the results of elastic modulus, tensile strength and elongation at break obtained from monotonic

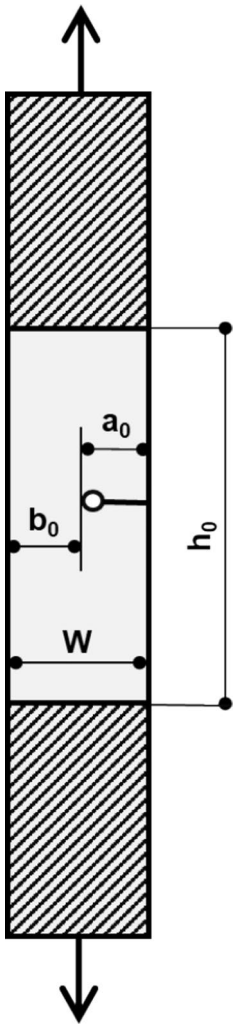

Fig. 1 Schematic representation of the SENT blunt-notched specimen used for the fracture tests (scale drawing)

tests, as well as residual elongations obtained from cyclic tests. The elastic modulus was evaluated as the slope of the line secant to the curve at the strain levels of 0.5% and 1.5%. The tensile strength and the elongation at break were calculated as the maximum stress and maximum elongation, respectively.

The elastic moduli of materials A and C are similar (taking into account the standard deviation of the results), and both are lower than the modulus of material B. This reflects the hardness levels, equal to 80 ShA for A and C and to 92 ShA for B (see Table 1). All materials deform several times their specimen length before failure occurs: A and B reach about 400% elongation at break, although the tensile strength in B is higher than in A, whereas C outperforms the other materials in terms of deformability (elongation at break is 710%) and reaches a stress level not very different from that of material B.

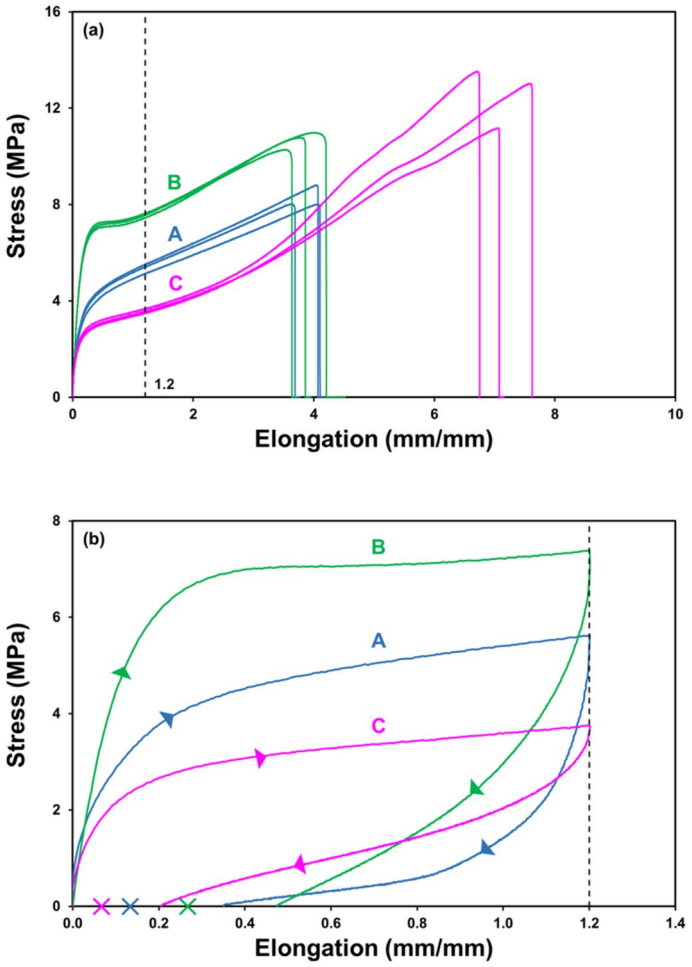

Fig. 2 Monotonic (**a**) and cyclic (**b**) nominal stress versus elongation curves from uniaxial tensile tests. In (**b**), the crosses on the elongation axis indicate the residual elongation at ∞ time measured for the three TPEs

Table 2 Tensile properties of the various materials. For each property evaluated from the monotonic tests, the mean value ± standard deviation from three test repetitions is reported

Mat	From monotonic tests			From cyclic tests (max elongation of 120%)	
	Elastic modulus, E [MPa]	Elongation at break, ε_{max} [%]	Tensile strength, σ_{max} [MPa]	Residual elongation [%]	Residual elongation at ∞ time [%]
A	40 ± 7	390 ± 24	8.3 ± 0.5	35.1	≈13
B	58 ± 1	377 ± 26	10.7 ± 0.4	47.5	≈27
C	34 ± 3	711 ± 45	12.6 ± 1.2	20.7	≈7

To put to evidence the material behaviour, cyclic tests (one single cycle, composed of the loading and unloading phases) were performed on virgin (undeformed) specimens. The stress-elongation curves are reported in Fig. 2b. The specimens were loaded until 120% of elongation and then unloaded at a lower rate, and the unloading curve was recorded as well. The maximum level of elongation was set in a region where the nonlinear behaviour is fully developed in all three materials (the minimum slope of the curve is reached slightly earlier) but before the start of the hardening phase. The elongation level reached immediately at the end of the downloading phase (residual elongation) is always lower than half of the maximum elongation achieved during the test. In other words, materials recover more than 50% of the applied deformation at the applied test rate. This is clear evidence of the elastic response of the materials, although not all the recovered deformation is purely elastic, as the downloading phase took between 2 and 3 min to occur, and viscoelastic deformations can also be a reason. As a proof of viscoelastic behaviour, specimens were removed from the test machine and left free to retract for ten weeks. After this time frame, the deformation of specimens compared to the virgin state was measured, and it is reported in Fig. 2b (as crosses on the elongation axis), as well as in Table 2. This residual elongation at ∞ time is lower than the deformation at the end of the unloading phase, putting to evidence the viscoelastic character of the materials. This residual elongation is considered irreversible and can take origin from plastic behaviour and/or from dissipative phenomena. Therefore, plasticity, here intended as the ability to accumulate non-recoverable deformations, was detected in the three different TPEs examined, to different extents. It is worth emphasising that this observation comes from the first loading cycle (one single cycle on undeformed materials). Both the tensile and fracture behaviours of TPEs were studied on virgin materials, at the first loading. It is reasonable to expect a different response after repeated (multiple) cycles; aspect outside the scope of this work, but which could be the subject of future studies.

Stationary fracture tests were carried out to investigate the applicability of the LSC to virgin TPEs. For each material, clamped SENT specimens with various crack lengths were tested, and the load-displacement curves obtained are reported in Fig. 3. As expected, for all the materials, by increasing the a_0/W ratio, the specimen compliance increases. In Fig. 3, the vertical dashed line indicates the level of displacement beyond which the data were not considered in the data processing due to possible fracture propagation (see in "Experimental" section).

For the determination of the S_{ij} parameter according to Eq. 3, the reference curve was identified for each TPE. This curve is shown in Fig. 3 as "j" and it corresponds to the specimen with crack length a_j. It is not relevant for the validity of the procedure which curve is selected as the reference one. For each TPE, all the other curves (corresponding to the specimens with crack length $a_{i\neq j}$) were used as the "i" curves. Operatively, firstly the initial elastic compliance, $C(b_0/W)$, corresponding to the uncracked and undeformed ligament length b_0, was calculated for each load-displacement curve from the slope of the load-displacement curve at the origin of the curve. Secondly, the displacement was converted into the plastic displacement via Eq. 2. It should be pointed out that Eq. 2 is originally developed for the elastic-plastic material behaviour of metals and that u_{pl} calculated

Fig. 3 Load, P, versus displacement, u, curves from stationary crack experiments on SENT specimens ▶ of material A (**a**), B (**b**) and C (**c**). For each specimen, the actual value of a_0/W is reported close to the curve. The vertical dashed line indicates the level of displacement beyond which the data were not considered in the data processing

with Eq. 2 includes all types of deformation, except the linear elastic one. For TPEs, u_{pl} includes nonlinear elastic, viscoelastic and irreversible strain contributions, and in this work, u_{pl} was renamed "nonlinear-elastic" displacement, u_{nle}. The choice to rename u_{pl}, done also by other researchers (see [37]), stems from the intention to frame the u_{pl} quantity in a more scientifically correct way, taking into account the peculiar behavioural characteristics of the materials under study. Furthermore, once the applicability of LSC is experimentally verified (as in the case of the TPE examined in this work), this allows to implicitly underline that having a purely elastoplastic response is not a necessary condition for the validity of LSC (which, from a theoretical point of view, is an assumption). Finally, the S_{ij} values at various u_{nle} levels were found for each pair (i, j) of curves, for each TPE. The load separation parameter curves, S_{ij} versus u_{nle}, of the various specimens were then plotted. They are shown in Fig. 4.

All the S_{ij} curves in Fig. 4 show a common trend: after an initial region where S_{ij} values are highly variable (evidenced in the grey background), they reach reasonably stable values over the u_{nle} domain examined. This is a clear indication that the LSC is applicable to TPEs, at least to the three TPE types examined in this work. The grey area at the beginning, which has already been seen in tests on metals and later on polymers, is the "unseparable" region. This is where the "plastic" pattern is still developing and the LSC does not apply. It is confined to a relatively limited region in the nonlinear elastic domain, and after a careful examination of the curves, for the determination of an average value of S_{ij} (see below), it was decided to consider an extension of the non-separable zone of 2 mm, irrespective of the TPE examined. Excluding the non-separable zone, the variation of S_{ij} with respect to the mean value generally remains below 5% for all the specimens examined, as an indication of the stability of S_{ij} curves, with the sole exception of the specimen with the highest a_0/W for materials A and C and the two specimens with the highest levels of a_0/W for material B.

When the TPE B was tested on the two specimens with the highest a_0/W values (a_0/W of 0.73 and 0.79), the process zone could be seen to go through the whole ligament of the specimen and reach the edge of the specimen. The load separation curves obtained for these two specimens are represented by dashed lines in Fig. 4 and, to exclude possible complications due to the edge effects just presented, these two curves have been omitted for the subsequent calculations.

The load separation parameter curves were then used to determine the geometry function, G (see Eq. 1). For each S_{ij} versus u_{nle} curve of Fig. 4, an average value of S_{ij} (indicated with $S_{ij,m}$) was calculated in the region where the curves maintain a stable value (above the grey region). For the specimen used as the reference one (with crack length a_j): $S_{jj,m} = 1$. Such values are plotted in Fig. 5 in a bi-logarithmic plot as a function of the $b_{0,i}/W$ ratio.

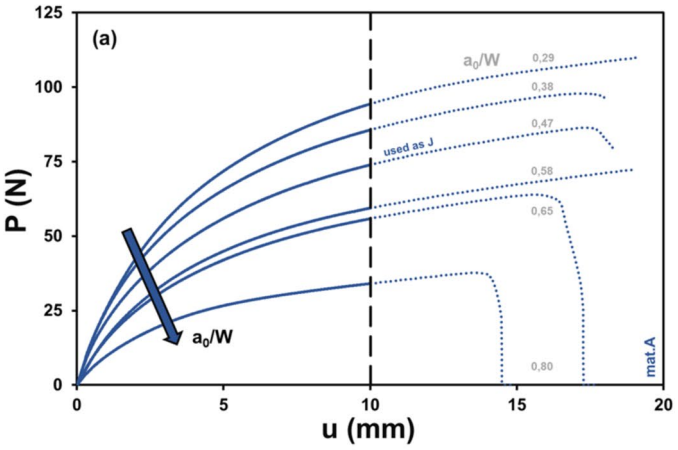
(a)
P (N)
u (mm)
a0/W
0,29
0,38
0,47
used as J
0,58
0,65
0,80
mat.A

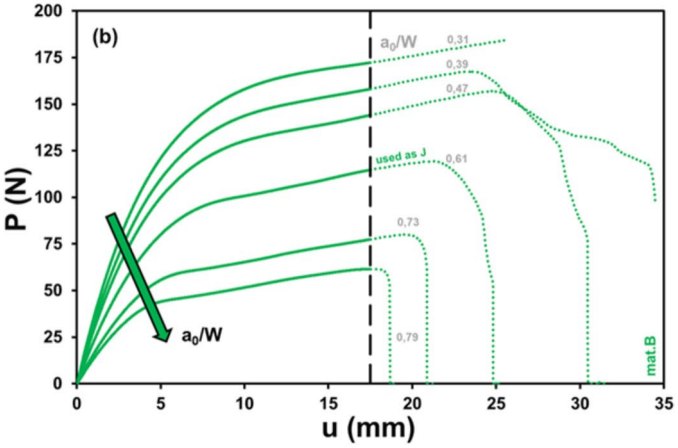
(b)
P (N)
u (mm)
a0/W
0,31
0,39
0,47
used as J
0,61
0,73
0,79
mat.B

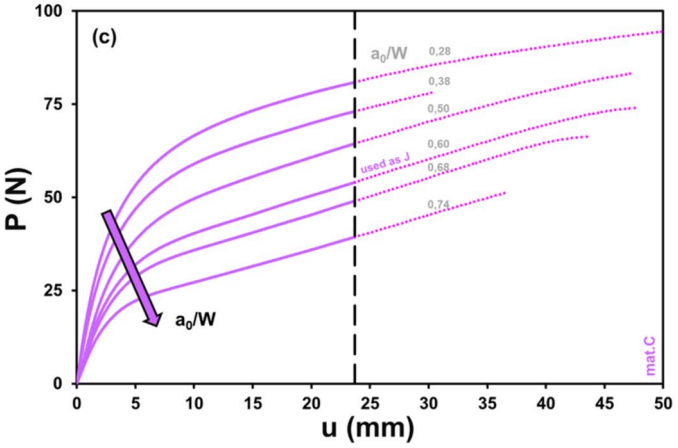
(c)
P (N)
u (mm)
a0/W
0,28
0,38
0,50
0,60
used as J
0,68
0,74
mat.C

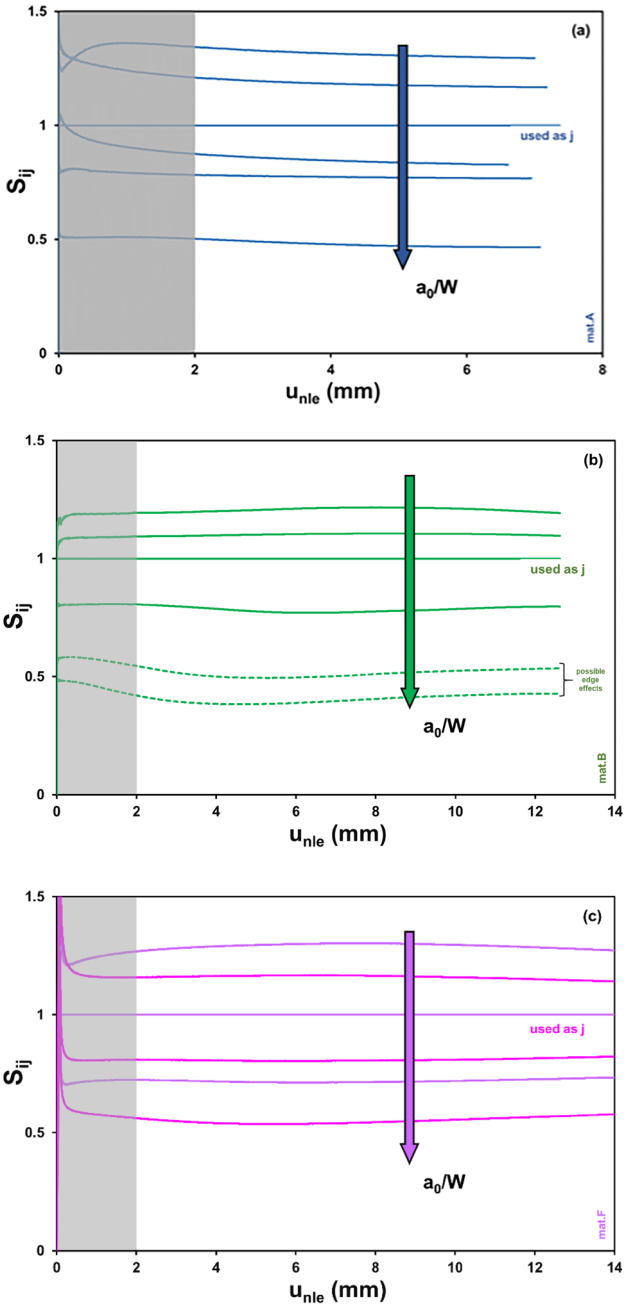

Fig. 4 Load separation parameter, S_{ij} versus u_{nle}, curves constructed for the various specimens of material A (**a**), B (**b**) and C (**c**). The grey region has been considered as the "unseparable" zone, and the data points within this area were not considered for the determination of $S_{ij,m}$ (see text). In (b), the dashed lines refer to specimens for which edge effects were observed during the tests

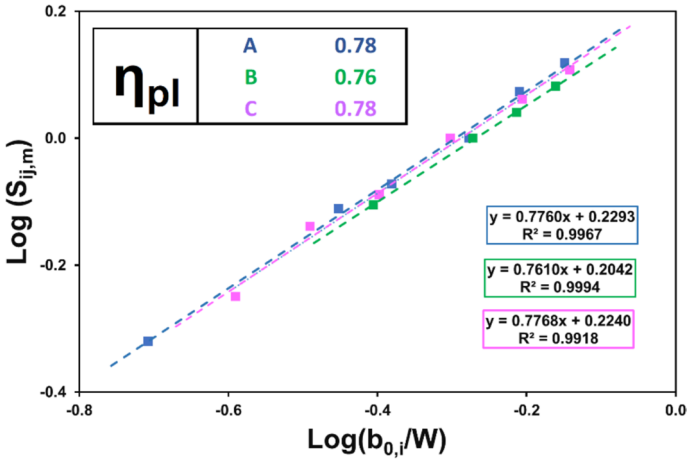

Fig. 5 Bi-logarithmic plot of $S_{ij,m}$ versus $b_{0,i}/W$ for the different TPEs examined. Datasets are fitted by linear regression lines (equations reported), and η_{pl} values are also displayed

For each TPE, experimental data of Fig. 5 follow a linear trend and therefore confirm the power-law expression of the geometry function (Eq. 5). Values of η_{pl} for each material were then obtained as the slope of the linear fitting (in the bi-logarithmic plot) of the experimental data and resulted in 0.78 for material A, 0.76 for material B, and 0.78 for material C. The fact that such values are quite close to each other confirms that the geometry function is independent of the material, as expected if the load separability is verified. Moreover, this evidence is further strengthened by the fact that similar values are reported in the literature for other materials but with similar geometry (clamped SENT thin specimens with an h_0/W ratio of 2, which is similar to h_0/W of 2.7 used in this work, and with a nominal thickness of 1 mm): Chandra et al. reported $\eta_{pl}=0.79$ for a steel sheet [38]; unpublished data by the authors reported $\eta_{pl}=0.76$ for a polyamide 6 (tested in slightly wet conditions). Literature results [37] show that even for thick SENT specimens η_{pl} is equal to 0.76.

Finally, as the geometry function was defined, the material deformation functions can be obtained by reversing Eq. 1 and making the geometry function explicit as follows:

$$H\left(\frac{u_{pl}}{W}\right)=\frac{P}{G\left(\frac{b}{W}\right)}=\frac{P}{\left(1-\frac{a}{W}\right)^{\eta_{pl}}} \tag{8}$$

However, the H function is commonly expressed by an alternative form given in stress dimensions and defined as "normalised load", P_N [8]:

$$P_N=\frac{P}{B\cdot W\cdot\left(1-\frac{a}{W}\right)^{\eta_{pl}}} \tag{9}$$

P_N versus u_{nle} is labelled the "material key curve". The material key curves obtained from each specimen tested (with the only exception of the two specimens of material B for which edge effects were clearly noticed) are reported in Fig. 6.

Material key curves, expressions of the material deformation function, H, are theoretically dependent only on material and constraint. The fact that, for each material, the material key curves obtained from test pieces with different a_0/W are very similar seems to suggest that, in the a_0/W range examined (with the sole exception of the two specimens of material B for which edge effects were clearly noticed), the different geometry (crack length) plays only a secondary role in the deformational response of the cracked specimen in the nonlinear-elastic region.

Conclusions

In this study, clamped SENT stationary crack experiments were carried out on blunt-notched specimens so that the crack could not propagate. The experiments were done under plane stress conditions and show that LSC seems to work for all three TPEs that were looked at. The three materials differ for both the chemical structure and the degree of plasticity they exhibit, here intended as the ability to accumulate non-recoverable deformations. As proof of the LSC validity, the load separation parameter, S_{ij}, was found to be constant over the whole nonlinear elastic displacement range investigated, except for a very limited region at small displacements. The geometry function $G(b/W)$ could be constructed and was found to be independent of the material and in line with literature results obtained for other classes of materials. It is of power-law type, whose exponent (that is, η_{pl}) keeps between 0.76 and 0.78. Because of the validity of the LSC, the material deformation functions were also obtained. They resulted to be different for the three materials investigated

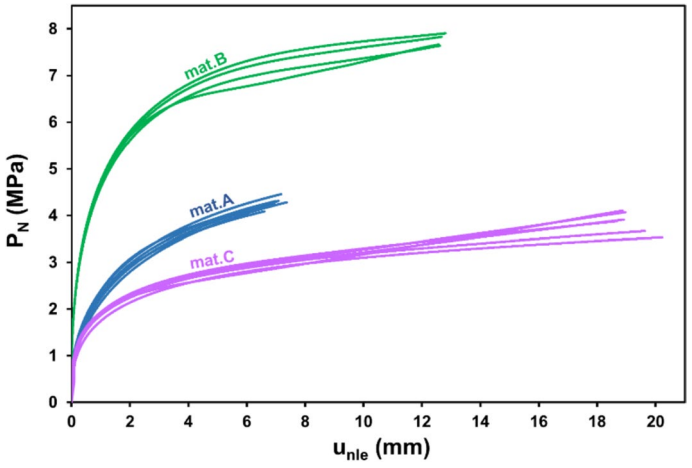

Fig. 6 Normalised load, P_N, versus u_{nle} curves ("material key curves") constructed for the various specimens of the different TPEs examined

and practically independent of the specimens' a_0/W ratio, showing that they do not depend on specimen geometry. Possible edge effects detected for material B suggest that attention should be paid to the choice of the fracture specimen dimensions. The research of possible relationships between the H function and the material's stress-strain response is underway.

Overall, the study suggests that the LSC is applicable to a range of TPE materials with varying chemical structures. This means that time-saving single-specimen techniques based on the LSC can be applied to reliably characterise fracture behaviour and evaluate the fracture toughness of TPE.

The next future studies will focus on the application of the LSC to sharp-notched specimens to identify the point of fracture initiation and obtain the material's fracture toughness from a single-specimen test, without the necessity either to construct the material crack growth resistance, J_R, curve (J versus crack extension) or to monitor the crack advancement.

In conclusion, this study contributes to the advancement of testing techniques for TPE materials and highlights the versatility and reliability of the LSC method in measuring their fracture properties.

Acknowledgements The authors are grateful to Univet S.r.l. (Rezzato, Brescia, Italy), Plastec S.r.l. (Gussago, Brescia, Italy) and Franplast S.p.A. (Provaglio d'Iseo, Brescia, Italy) for kindly supplying the materials tested in this study. A special thanks to Plastec S.r.l. also for the preparation of the plates via injection moulding. The authors are also grateful to Ms. Isabella Peroni and Ms. Gloria Spagnoli of Dipartimento di Ingegneria Meccanica e Industriale of Università degli Studi di Brescia (Brescia, Italy) for the support in the execution of the DSC tests.

Author contributions S.G. conducted laboratory experiments and data analysis. S.G., J.A. and S.A. contributed to the literature review. S.G., S.A. and F.Ba. wrote the main manuscript text and prepared all the figures and tables. All authors reviewed the manuscript.

Funding No funding was received for conducting this study.

Data availability No datasets were generated or analysed during the current study.

Declarations

Conflict of interest The authors have no competing interests to declare that are relevant to the content of this article.

Open Access This article is licensed under a Creative Commons Attribution 4.0 International License, which permits use, sharing, adaptation, distribution and reproduction in any medium or format, as long as you give appropriate credit to the original author(s) and the source, provide a link to the Creative Commons licence, and indicate if changes were made. The images or other third party material in this article are included in the article's Creative Commons licence, unless indicated otherwise in a credit line to the material. If material is not included in the article's Creative Commons licence and your intended use is not permitted by statutory regulation or exceeds the permitted use, you will need to obtain permission directly from the copyright holder. To view a copy of this licence, visit http://creativecommons.org/licenses/by/4.0/.

References

1. Cherepanov GP (1967) Crack propagation in continuous media. J Appl Math Mech 31(3):503–512. https://doi.org/10.1016/0021-8928(67)90034-2
2. Rice JR (1968) A path independent integral and the approximate analysis of strain concentration by notches and cracks. J Appl Mech 35:379–386. https://doi.org/10.1115/1.3601206
3. Anderson TL (2017) Fracture mechanics: fundamentals and Applications, 4th edn. CRC Press, Boca Raton
4. Begley JA, Landes JD (1972) The J Integral as a Fracture Criterion. ASTM Spec Tech Publ STP 514:1–20. https://doi.org/10.1520/STP38816S
5. Landes JD, Begley JA (1972) The Effect of Specimen Geometry on JIc. ASTM Spec Tech Publ STP 514:24–39. https://doi.org/10.1520/STP38817S
6. Ernst HA, Paris PC, Landes JD (1981) Estimations on J-integral and tearing modulus T from a single specimen test record. ASTM Spec Tech Publ. https://doi.org/10.1520/STP28814S
7. Sharobeam MH, Landes JD (1991) The load separation criterion and methodology in ductile fracture mechanics. Int J Fract 47:81–104. https://doi.org/10.1007/BF00032571
8. Sharobeam MH, Landes JD (1993) The load separation and ηpl development in precracked specimen test records. Int J Fract 59:213–226. https://doi.org/10.1007/BF00012362
9. Bernal CR, Cassanelli AN, Frontini PM (1995) A simple method for J-R curve determination in ABS polymers. Polym Test 14:85–96. https://doi.org/10.1016/0142-9418(95)90616-O
10. Bernal CR, Cassanelli AN, Frontini PM (1996) On the applicability of the load separation criterion to acrylonitrile/butadiene/styrene terpolymer resins. Polymer (Guildf) 37:4033–4039. https://doi.org/10.1016/0032-3861(96)00232-7
11. Bernal CR, Montemartini PE, Frontini PM (1996) The use of load separation criterion and normalization method in ductile fracture characterization of thermoplastic polymers. J Polym Sci B Polym Phys 34:1869–1880. https://doi.org/10.1002/(SICI)1099-0488(199608)34:11%3c1869::AID-POLB4%3e3.0.CO;2-N
12. Morhain C, Velasco JI (2001) Determination of j-r curve of polypropylene copolymers using the normalization method. J Mater Sci 36:1487–1499. https://doi.org/10.1023/A:1017500930544
13. Morhain C, Velasco JI (2002) J-R curve determination of magnesium hydroxide filled polypropylene using the normalization method. J Mater Sci 37:1635–1644. https://doi.org/10.1023/A:1014944729912
14. Salazar A, Rodríguez J (2008) The use of the load separation parameter Spb method to determine the J-R curves of polypropylenes. Polym Test 27:977–984. https://doi.org/10.1016/J.POLYMERTESTING.2008.08.013
15. Baldi F, Agnelli S, Riccò T (2010) On the applicability of the load separation criterion in determining the fracture resistance (J Ic) of ductile polymers at low and high loading rates. Int J Fract 165:105–119. https://doi.org/10.1007/S10704-010-9510-9
16. Landes JD, Zhou Z (1993) Application of load separation and normalization methods for polycarbonate materials. Int J Fract 63:383–393. https://doi.org/10.1007/BF00013045
17. Zhou Z, Landes JD, Huang DD (1994) J-r curve calculation with the normalization method for toughened polymers. Polym Eng Sci 34:128–134. https://doi.org/10.1002/PEN.760340209
18. Baldi F, Riccò T (2005) High-rate j-testing of toughened polyamide 6/6: applicability of the load separation criterion and the normalization method. Eng Fract Mech 72:2218–2231. https://doi.org/10.1016/J.ENGFRACMECH.2005.02.002
19. Wainstein J, Frontini PM, Cassanelli AN (2004) J-R curve determination using the load separation parameter Spb method for ductile polymers. Polym Test 23:591–598. https://doi.org/10.1016/J.POLYMERTESTING.2003.10.010
20. Agnelli S, Baldi F, Blackman BRK et al (2015) Application of the load separation criterion in J-testing of ductile polymers: A round-robin testing exercise. Polym Test 44:72–81. https://doi.org/10.1016/J.POLYMERTESTING.2015.03.019
21. Baldi F, Agnelli S, Andena L et al (2020) Determination of the fracture resistance of ductile polymers: the ESIS TC4 recent experience. Mater Perform Charact 9:675–687. https://doi.org/10.1520/MPC20190175
22. European Structural Integrity Society, ESIS Home Page. https://www.esis.site/. Accessed 4 Jun 2025

23. ISO - International Organization for Standardization, ISO Home Page. https://www.iso.org/home.html. Accessed 4 Jun 2025
24. Drobny JG (2014) Handbook of thermoplastic elastomers. Elsevier, Oxford
25. White JR, De SK (2001) Rubber Technologist's Handbook. Rapra, Shrewsbury
26. Parenteau T, Bertevas E, Ausias G et al (2014) Characterisation and micromechanical modelling of the elasto-viscoplastic behavior of thermoplastic elastomers. Mech Mater 71:114–125. https://doi.org/10.1016/J.MECHMAT.2013.06.010
27. Cho H, Mayer S, Pöselt E et al (2017) Deformation mechanisms of thermoplastic elastomers: stress-strain behavior and constitutive modeling. Polymer (Guildf) 128:87–99. https://doi.org/10.1016/J.POLYMER.2017.08.065
28. Sbrescia S, Ju J, Engels T et al (2021) Morphological origins of temperature and rate dependent mechanical properties of model soft thermoplastic elastomers. J Polym Sci 59:477–493. https://doi.org/10.1002/pol.20200791
29. Lesser AJ, Jones NA (2000) Fracture behavior of dynamically vulcanized thermoplastic elastomers. J Appl Polym Sci 76:763–770. https://doi.org/10.1002/(SICI)1097-4628(20000509)76:6%3c763::AID-APP1%3e3.0.CO;2-O
30. Major Z, Isasi M, Schwarz T (2010) Characterization of the fracture and fatigue behavior of thermoplastic elastomer materials. Key Eng Mater 417–418:789–792. https://doi.org/10.4028/WWW.SCIENTIFIC.NET/KEM.417-418.789
31. Mars WV, Ellul MD (2017) Fatigue characterization of a thermoplastic elastomer. Rubber Chem Technol 90:367–380. https://doi.org/10.5254/RCT.17.83780
32. Maspoch ML, Santana OO, Grando J et al (1997) The essential work of fracture of a thermoplastic elastomer. Polym Bull 39:249–255. https://doi.org/10.1007/S002890050145
33. Sumpter JDG, Turner CE (1976) Method for Laboratory Determination of Jc. ASTM Spec Tech Publ STP 601:3–18. https://doi.org/10.1520/STP28634S
34. Paris PC, Ernst H, Turner CE (1980) A J-integral approach to development of η-factors. ASTM Spec Tech Publ STP 700:338–351. https://doi.org/10.1520/STP36979S
35. ISO 868:2003 - Plastics and ebonite — Determination of indentation hardness by means of a durometer (Shore hardness)
36. ISO 37:2024 - Rubber, vulcanized or thermoplastic — Determination of tensile stress-strain properties
37. Martinez M, Lopez R, Rodríguez J, Salazar A (2022) Evaluation of the structural integrity of solid rocket propellant by means of the viscoelastic fracture mechanics approach at low and medium strain rates. Theor Appl Fract Mech 118:103237
38. Chandra SK, Sarkar R, Choudhury S et al (2021) Determination of ηp factor for clamped SENT thin sheet specimens of an interstitial free steel. Int J Fract 227:137–152. https://doi.org/10.1007/S10704-020-00493-9

Publisher's Note Springer Nature remains neutral with regard to jurisdictional claims in published maps and institutional affiliations.